

Irreversibility limits of the Abrikosov and Josephson flux dynamics in homogeneous and granular high- T_C superconductors

V. N. Vieira, J. P. da Silva, and J. Schaf*

Instituto de Física - Universidade Federal, do Rio Grande do Sul-UFRGS, CEP 91501-970, Porto Alegre-RS, Brazil

(Received 15 December 2000; revised manuscript received 5 March 2001; published 14 August 2001)

The magnetic irreversibility of a high-quality $\text{YBa}_2\text{Cu}_3\text{O}_{7-\delta}$ single crystal and of the granular superconductors $\text{YBa}_{1.5}\text{Sr}_{0.5}\text{Cu}_3\text{O}_{7-\delta}$ and $\text{YBa}_{1.75}\text{Sr}_{0.25}\text{Cu}_3\text{O}_{7-\delta}$ single crystals and the polycrystalline $\text{YBa}_{1.75}\text{Sr}_{0.25}\text{Cu}_3\text{O}_{7-\delta}$ sample in two different oxygen states was determined in great detail, as a function of applied field up to 5 T from zero-field-cooled and field-cooled dc magnetization. While the T_{irr} data of the pure single crystal are well described by the power law, predicted by the flux-creep models, in the whole field range, those of the granular superconductors adhere to this power law only in the high-field region. In a low-field region two quite different regimes take place: In the lowest fields the data obey a de Almeida-Thouless-like power law and above a sharp crossover field they follow a Gabay-Toulouse-like power law. These low-field features are acknowledged as the signature of a frustrated system.

DOI: 10.1103/PhysRevB.64.094516

PACS number(s): 74.25.Ha, 74.62.Dh, 74.72.Bk, 74.80.Bj

I. INTRODUCTION

The magnetic properties of the high- T_C oxide superconductors (HTSC) are largely determined by their magnetic irreversibility, which, in turn, is intimately related to the nature and topology of the superconducting state. Although intensely studied since the discovery of the HTSC, the origin of the magnetic irreversibility is still a matter of strong controversy. The theoretical interpretation has been attempted along several lines. A first one, launched in the pioneering work of Müller and co-workers,¹ sees in the magnetic irreversibility line of the HTSC the signature of a genuine phase transition of an inhomogeneous, disordered, and frustrated granular superconductor. A second line tries to describe it as a conventional flux-creep phenomenon, analogous to that of the homogeneous low-temperature superconductors.² However, the assumptions underlying this approach, though well suited for conventional superconductors, are in clear conflict with the two-step resistive transition, observed in all but the best $\text{YBa}_2\text{Cu}_3\text{O}_{7-\delta}$ single crystals, which thoroughly shows that practically all the HTSC are granular³⁻⁶ and not homogeneous superconductors, their magnetic behavior involving the metastability of the intergranular as well as of the intra-granular flux dynamics, which are quite different. Therefore the conventional flux-creep theories can in general not account for the magnetic irreversibility in the whole field range.

The superconducting granularity of the HTSC results not only from the polycrystallinity. Due to the very short coherence length of their Ginsburg-Landau (GL) order parameter, any defect of the crystal lattice introduces a strong local depression of the superconducting order parameter⁷ and normally leads to granularity even in single crystals.⁸ Twinning planes and dislocations may in general separate a superconducting grain into subgrains that remain only weakly connected. Any increase in the number and size of such defects results in the increase of the granularity. Oxygen depletion has been verified⁵ by resistivity and magnetization to strongly debilitate the weak links and to reinforce the granu-

lar character of pure polycrystalline $\text{YBa}_2\text{Cu}_3\text{O}_{7-\delta}$. On the other hand replacing in this system Ba by Sr strongly increases the twinning⁹ and reduces the coherence length,^{10,11} thereby sharpening the topology of the GL order parameter and increasing the granular character of the superconductor.

In nearly perfect $\text{YBa}_2\text{Cu}_3\text{O}_{7-\delta}$ single crystals, whose superconducting granularity is vanishingly low, the Abrikosov flux is the only one relevant. Therefore the flux dynamics is relatively simple and can effectively be understood in terms of the conventional flux creep.¹² The magnetic irreversibility limit of such homogeneous superconductors as a function of the applied field [$T_{irr}(H)$] is well described by the power law arising within the flux-creep (fc) theories:^{2,13-18}

$$H(T) = H_0^{fc} (1 - t^{fc})^\alpha \quad (\alpha = \frac{3}{2}). \quad (1)$$

Here $t^{fc} = T_{irr}^{fc}(H)/T_{irr}^{fc}(0)$, and H_0^{fc} as well as $T_{irr}^{fc}(0)$ are fitting parameters. This power law is sometimes referred to as the universal function.

The flux dynamics in granular HTSC is however much more complex once it comprises the dynamics of two kinds of magnetic flux. However, in many circumstances the flux dynamics is dominated by only one or the other kind of flux, when they can be studied separately. For instance the critical field for penetration of Josephson fluxons (H_{c1J}) into the intergrain spaces is much weaker than that for penetration of Abrikosov fluxons into the grains themselves (H_{c1g}) once the size of the superconducting grains is not much larger than the penetration length of the field. Moreover the motion of the Josephson flux is opposed only by the discrete weak couplings between the grains. Therefore its activation energy is significantly lower than that of the Abrikosov flux. Effectively the motion of the Josephson flux has been verified to begin tens of degrees below the magnetic irreversibility limit and to dominate flux dynamics in the low fields and low temperatures.¹⁹ This occurs because the existing intragrain Abrikosov flux is not activated or because it isn't present at all. Moreover this intergrain flux dynamics is expected to be strongly marked by the frustrated grain coupling physics.²⁰ Therefore the behavior of the magnetic irreversibility

$T_{irr}(H)$ of polycrystalline samples in low fields^{5,19,21} may be characterized by the intergrain flux. It in fact totally resembles that of the well-known magnetic irreversibility line of spin glasses,²² characterized in low fields by a (AT) de Almeida-Thouless²³ like line

$$H(T) = H_0^{AT} (1 - t^{AT})^\alpha \quad (\alpha = \frac{3}{2}), \quad (2)$$

where $t^{AT} = T_{irr}^{AT}(H)/T_{irr}^{AT}(0)$, and H_0^{AT} and $T_{irr}^{AT}(0)$ are fitting parameters. Müller and co-workers remarked on this in their pioneering work of LaBaCuO.¹ Although the mathematical form of Eqs. (1) and (2) are identical, their physical origins are completely different.

In many subsequent and highly detailed studies of the magnetic irreversibility^{5,6,10,11,21,24} it was however found that in the $T_{irr}(H)$ data of granular $\text{YBa}_2\text{Cu}_3\text{O}_{7-\delta}$ and BiSrCaCuO superconductors, although obeying a AT-like power law in the very lowest fields, they consistently deviate from this power law above a crossover field of nearly 0.5 kOe. Moreover the behavior of these $T_{irr}(H)$ data of a polycrystalline $\text{YBa}_2\text{Cu}_3\text{O}_{7-\delta}$ sample, in several oxygen-depleted states,⁵ a $\text{Bi}_2\text{Sr}_2\text{Ca}_2\text{Cu}_3\text{O}_y$ sample,²⁴ and a doped $\text{YBa}_2\text{Cu}_{2.98}\text{Zn}_{0.02}\text{O}_{7-\delta}$ superconductor, above the crossover field, could be well fitted by a (GT) Gabay-Toulouse²⁵ like power law

$$H = H_0^{GT} (1 - t^{GT})^\alpha \quad (\alpha = \frac{1}{2}), \quad (3)$$

where $t^{GT} = T_{irr}^{GT}(H)/T_{irr}^{GT}(0)$, and H_0^{GT} and $T_{irr}^{GT}(0)$ are fitting parameters.

The occurrence of AT and GT power-law behaviors of the magnetic irreversibility and the AT-GT crossover at a few hundred oersted is long known²² to occur in spin glasses, where the origin of this crossover is quite well understood theoretically in terms of an Ising-Heisenberg or Ising-XY dimensionality transformation. The crossover occurs when the external applied field collapses the random local anisotropy fields.²⁶ However, the occurrence of a AT-GT-type crossover of $T_{irr}(H)$ in granular oxide superconductors is certainly intriguing and deepens even much more the analogy between the granular oxide superconductors and the spin glasses, raising a number of challenging questions.

In very strong fields ($H > 10$ kOe) and high-enough temperatures the amplitude of the phase fluctuations of the GL order parameter becomes high enough to uncouple the grains, permitting the field to circulate reversibly between them. Within these field and temperature conditions the superconducting grains contain a number of Abrikosov vortices, whose dynamics is governed by a physics much different from that of the Josephson flux. Abrikosov flux dynamics is thus expected to dominate the magnetic irreversibility in high fields.^{2,13-18}

In order to test these hypotheses and to confirm the existence of the different low-field regimes as well as to obtain the form of the magnetic irreversibility line in all the different field regions, we have measured precisely the magnetic irreversibility for samples with very different superconducting granularities: A pure and high-quality $\text{YBa}_2\text{Cu}_3\text{O}_{7-\delta}$ single crystal with vanishing granularity, two doped strongly twinned $\text{YBa}_{2-x}\text{Sr}_x\text{Cu}_3\text{O}_{7-\delta}$ ($x = 0.25$ and 0.5) single crys-

als with intermediate granularity, and a strongly granular $\text{YBa}_{1.75}\text{Sr}_{0.25}\text{Cu}_3\text{O}_{7-\delta}$ polycrystalline sample with two oxygen states. The granular superconducting character of all these materials is well known from previous electric resistivity and magnetic-susceptibility studies^{3,5,6,10,11} and were confirmed here once more. Apparently the granularity relevant to the magnetic irreversibility is quite generic and not specific to certain kinds of defects.

II. EXPERIMENTAL TECHNIQUES

The polycrystalline $\text{YBa}_{1.75}\text{Sr}_{0.25}\text{Cu}_3\text{O}_{7-\delta}$ samples were prepared by calcination of the pure oxides and carbonates in air, pressed into a pellet, and sintered at 950 °C with subsequent slow cooling from 750 to 650 °C. Oxygen saturation was achieved by slowly cooling in oxygen atmosphere (1 atm) from 450 °C to 250 °C over three days. Specimens were cut from the pellet in the form of long parallelepipeds, respectively, 2.2, 0.75, and 0.55 mm³ for magnetic and transport measurements. The oxygen depletion in the polycrystalline sample was performed by heating to 380 °C during 45 min in a vacuum and controlling by weight loss. We observed that the rate of oxygen loss of the Sr-doped samples is about ten times higher than in pure YBaCuO . This assures, in our view, that oxygen depletion does not significantly change the relative oxygen distribution with respect to that of the virgin sample. The densities of the samples were 5.33 g/cm³ and 5.29 g/cm³, respectively, before and after oxygen depletion. The pure $\text{YBa}_2\text{Cu}_3\text{O}_{7-\delta}$ and the doped $\text{YBa}_{1.5}\text{Sr}_{0.5}\text{Cu}_3\text{O}_{7-\delta}$ and $\text{YBa}_{1.75}\text{Sr}_{0.25}\text{Cu}_3\text{O}_{7-\delta}$ single crystals were grown in CuO flux in ZrO_2 trays by slowly lowering the temperature from 1020 °C to 880 °C over 18 h and subsequent slow cooling through 700 °C. Oxygenation of all the single crystals was made in a flowing oxygen atmosphere at 450 °C over ten days and subsequent slow cooling. The single crystals all had a platelet shape of a very homogeneous appearance with a nearly rectangular form about 1 mm² in area and nearly 0.07 mm in thickness. X-ray diffraction revealed no strange phases in all of the samples and examination of the doped single crystals with polarized light microscopy showed a high density of orthogonal twinning planes, as also reported by the authors of Ref. 9. It may also be remarked that the form, shape, and even the size and orientation of the samples with respect to the applied field, although relevant for the demagnetizing field and precision of the measurements, do not significantly affect the functional form of the irreversibility line.

Our main experimental work was aimed at measuring the magnetic irreversibility with dc magnetization methods, but electric resistivity measurements were also made in order to get a better insight on the granularity of our samples. While precise electric resistivity measurements can provide detailed information on the superconducting transition within the grains, the grain coupling process, and fluctuation conductivity, dc magnetization is especially suited to provide information on the critical fields, critical currents, flux mobility, relaxation, and magnetic irreversibility. Our magnetization measurements were made under applied fields up to 50 kOe by using a superconducting quantum interference device

MPMS-XL magnetometer from Quantum Design and the resistivity measurements were made with a very precise low current low-frequency ac experimental setup, where a lock-in amplifier is used as a null detector, having a sensitivity of $10^{-5} \Omega$ and a temperature resolution of 0.02 K.

III. EXPERIMENTAL RESULTS

A. Magnetoconductivity

Granular HTSC, having a well-defined superconducting transition temperature, in general display a visible two stage resistive transition $\rho(T)$ and correspondingly $d\rho/dT$ displays a peak and a hump or shoulder at the lower-temperature side of the peak.²¹ While the peak marks the pairing critical temperature T_C within the grains, the shoulder is related to the grain coupling and the coherence transition of the granular system. The weak links that connect the superconducting grains are well known²⁰ to be very sensitive to magnetic fields. An applied field distorts the phase of the GL order parameter and weakens the coupling energy between the grains, while leaving almost intact the superconducting transition within the grains. These effects strongly extend the lower-temperature foot of the resistive transition, enlarging the hump of the coherence transition in $d\rho/dT$, but leaving the main peak of the intragrain transition sharp and at the same position. Figure 1 exemplifies the resistive transitions and the corresponding temperature derivatives of a granular and a homogeneous superconductor, respectively, by our polycrystalline sample and the pure $\text{YBa}_2\text{Cu}_3\text{O}_{7-\delta}$ single crystal. The fact that the resistive transition of the pure single crystal occurs in one unique step and its temperature derivative gives only a single and sharp peak shows that this sample has a vanishing granularity. The other samples exhibit a two-step resistive transition, the corresponding temperature derivative displaying a sharp peak with a hump at its lower-temperature side. These are the well-known features of the granular superconductors. It can also be observed that low applied fields up to 0.6 kOe, while not affecting visibly the main intragranular transition, do strongly enlarge the hump of the coherence transition, demonstrating the sensitivity of the grain couplings to applied field.

B. Magnetic irreversibilities

The magnetic irreversibility limit [$T_{irr}(H)$] was measured within a precision of 0.5 K or better for a large number of applied fields from 0.003 to 50 kOe for all of our samples. The used method consisted of cooling the sample first under zero field, measuring the dc magnetization (M_{ZFC}) under stable field, while slowly warming (0.2 K/min or less) to a temperature well above T_C , and next measuring the magnetization (M_{FC}) while slowly cooling back under the same field and subtracting M_{ZFC} from M_{FC} . The temperature point where the difference data lift off from the zero base line, defined by the upper temperature data, is the irreversibility limit T_{irr} . To give an overview of our data analysis, we present in Fig. 2 some arbitrarily chosen examples of difference data. The arrows indicate the irreversibility limit for these cases and the insets show the corresponding M_{ZFC}

and M_{FC} data. It is important to note that in general locating the irreversibility limit directly from the M_{ZFC} and M_{FC} data is liable to be arbitrary as in general these curves approximate asymptotically. Difference data are much more safe. Plotting the T_{irr} data for the whole field range in a $H-T$ diagram defines the irreversibility line of the sample. The magnetic irreversibility data of our $\text{YBa}_{1.75}\text{Sr}_{0.25}\text{Cu}_3\text{O}_{7-\delta}$ polycrystalline sample are displayed in Fig. 3 for two oxygen states of the sample ($\delta \approx 0.0$ and 0.3). The continuous lines through the low-field data are fitted with de Almeida-Thouless-like lines [Eq. (2)] while the high-field data are fitted with the power law of the flux-creep model [Eq. (1)]. The dashed line through the high-field data at the right is a guide to the eye.

Figure 4 displays the $T_{irr}(H)$ data of the pure $\text{YBa}_2\text{Cu}_3\text{O}_{7-\delta}$ and the two Sr-doped single crystals together with those of the Sr-doped polycrystalline sample in an oxygen-depleted state. The single-crystal data are for $\vec{H} \parallel \hat{c}$. Except for the different slopes, the overall profiles of the irreversibility lines in Fig. 4 all look very similar. It in fact is largely defined by the behavior of the $T_{irr}(H)$ data in the major high-field region, where they all follow the so-called universal function of the flux-creep model, Eq. (1), shown in the figure as a continuous line. In the particular case of the pure $\text{YBa}_2\text{Cu}_3\text{O}_{7-\delta}$ single crystal, this behavior rigorously prevails in the whole field range. If the density of our irreversibility data were poor, as in most reported irreversibility studies, it would be very easy to overlook the low-field structure and to extend the universal function through the whole field range for all the samples. However, due to the precision and the number of $T_{irr}(H)$ data points in Fig. 4, even an inattentive look shows that the data of the granular samples fall systematically off the high-field regime in the low-field region. We highlight these low-field features in Fig. 5 where it becomes clear that the flux-creep regime extends down to zero field in the case of the pure single crystal. However in the case of the granular samples two different and well-defined regimes become systematically apparent. In the very lowest-field region the data define the well-known AT-like line [Eq. (2)] for all the granular samples. When the field value increases beyond about 0.7 kOe, $T_{irr}(H)$ changes abruptly its slope and bends in a sense opposite to that of the AT-like line. This intermediate-field regime is well fitted by a GT-like line, Eq. (3), for all the granular samples. In the case of the polycrystalline samples this GT-like behavior extends even up to about 10 kOe. The transition to the high-field regime is not abrupt and we see in it the hegemonic competition between the intergranular and intragranular flux dynamics. We list in Table I the values of the fitting parameters in the various field regions.

IV. DISCUSSION

In the homogeneous low-temperature superconductors, flux dynamics is described by the conventional flux-creep theories. The behavior of $T_{irr}(H)$ of very good $\text{YBa}_2\text{Cu}_3\text{O}_{7-\delta}$ single crystals according to the power law, Eq. (1), in the whole field range indicates that this flux-creep approach may also be valid in the case of very homogeneous

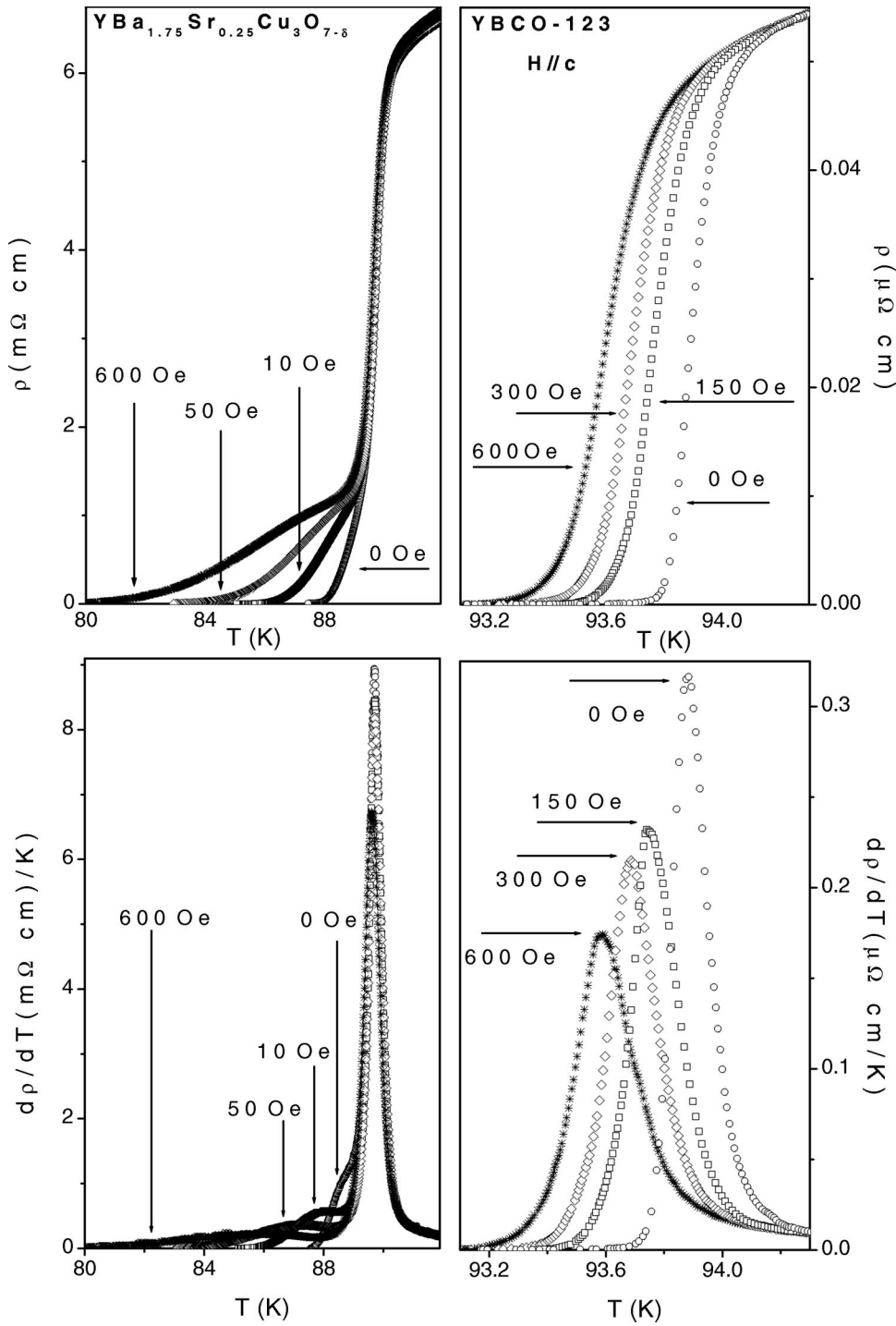


FIG. 1. The characteristic resistive transitions and temperature derivatives of granular (left) and homogeneous (right) superconductors represented, respectively, by our $YBa_{1.75}Sr_{0.25}Cu_3O_{7-\delta}$ polycrystalline sample and the pure $YBa_2Cu_3O_{7-\delta}$ single crystal. Notice the very different temperature scales.

HTSC.^{2,13-18,27} However some authors²⁸⁻³¹ found such a behavior ($\alpha = \frac{3}{2}$) of $T_{irr}(H)$ only in a low-field region. In higher fields their data assume the behavior of a melting line ($\alpha = 2$) and still others³²⁻³⁴ found a melting line in the whole field region. Many of these works however have very poor resolution especially in the low-field region. Moreover the determination of the irreversibility limit is in general purely visual on the raw data, which may lead to important erraticity.

The $T_{irr}(H)$ data of our granular superconductors adhere to the power-law regime, Eq. (1), only in relatively high

fields (typically above 10 kOe), where the intragrain flux dynamics is known to be dominant and neatly deviate from this regime in a low-field region, where the intergrain flux dynamics dominates. The behavior of the $T_{irr}(H)$ data is clearly AT-like [Eq. (2)] in the lowest fields and GT-like [Eq. (3)] above a crossover field, which are the well-known signatures of disordered and frustrated systems. Therefore the superconducting-glass^{1,5,20,35-37} or vortex-glass³⁸⁻⁴² models, which have entries for disorder and frustration, are the obvious scenario within which understanding for these low-field features must be sought. In fact these two models focus

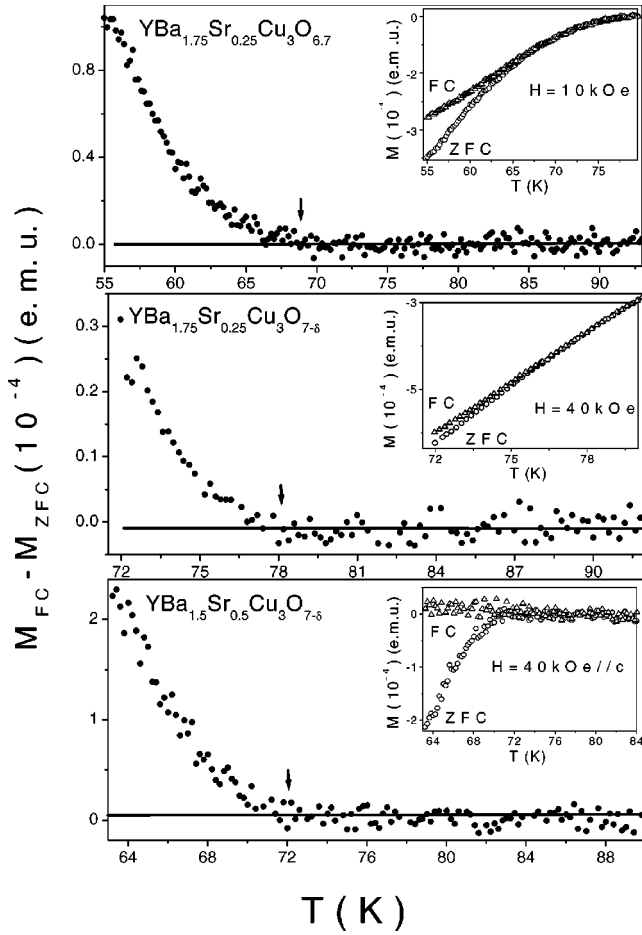


FIG. 2. Examples of difference data and the respective M_{ZFC} and M_{FC} curves (insets), chosen between the less favorable cases to emphasize the advantage of using difference data arrays to determine the irreversibility limit.

on different aspects of the same highly inhomogeneous superconductors. While the former emphasizes the jagged topology of the superconducting order parameter, the latter focuses on the respective random pinning and the consequent distortion of the flux-line lattice.

A superconducting glass may be conceived as a highly inhomogeneous superconductor or simply as a weakly coupled disordered superconducting grain aggregate under applied field. An irregular and weakly coupled grain network is usually described in terms of the effective Hamiltonian^{5,20,35–37,43,44}

$$H = -2e^2 \sum_{ij} n_i n_j C_{ij}^{-1} - \sum_{\langle i,j \rangle} J_{ij} \cos(\theta_i - \theta_j - A_{ij}). \quad (4)$$

Here the first term in the right-hand side represents the Coulomb energy, where C_{ij} are the elements of the capacitance matrix, and n_i (n_j) is the number of pairs on grain i (j). The second term is the Josephson coupling term, where the J_{ij} are the phase coupling energies between neighboring grains i and j and $\theta_i - \theta_j$ is the difference of the respective phases of the GL order parameter. The n_i and θ_j are canonically con-

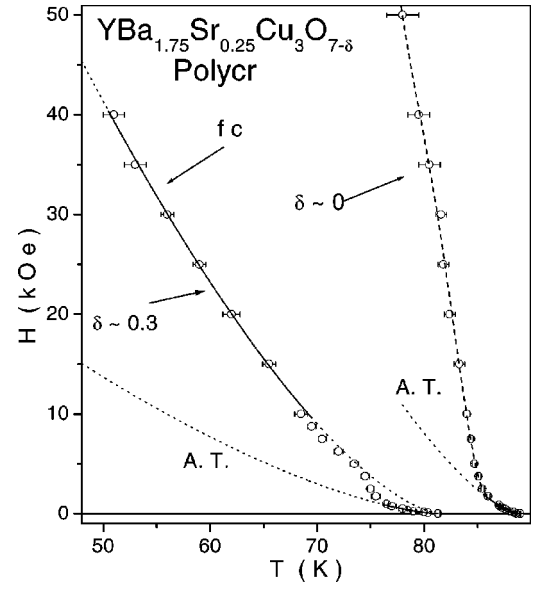


FIG. 3. The irreversibility data of our polycrystalline sample in the oxygen-saturated and oxygen-depleted state. The continuous line (A.T.) through the low-field data are fitted with Eq. (2); the one (f.c.) through the high-field data is fitted with Eq. (1). The dashed line through the high-field data at the right-hand side is a guide to the eye.

jugate variables satisfying the commutation rule $[n_i, e^{\theta_j}] = \delta_{ij} e^{\theta_j}$ and A_{ij} are the phase displacements

$$A_{ij} = \frac{2\pi}{\phi_0} \int_i^j \vec{A} \cdot d\vec{l} \quad (5)$$

introduced by the vector potential \vec{A} along the weak links between grains i and j . This equation shows that the applied

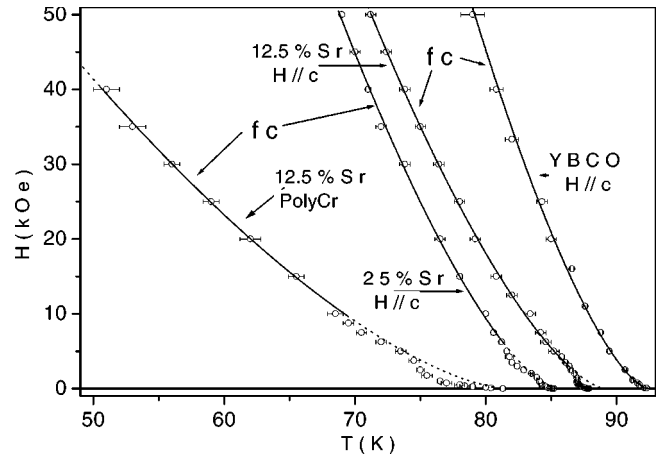


FIG. 4. From right to left, the $T_{irr}(H)$ data of the pure $\text{YBa}_2\text{Cu}_3\text{O}_{7-\delta}$ single crystal of two $\text{YBa}_2\text{Cu}_3\text{O}_{7-\delta}$ single crystals having Ba substituted by Sr in the indicated proportions and of the Sr-doped and oxygen-depleted polycrystalline sample. The continuous lines (f.c.) are fitted with the power law Eq. (1) [see fitting parameters in Table I]. Notice the low-field structure that is absent in the pure single crystal and increases with increasing granular character of the samples.

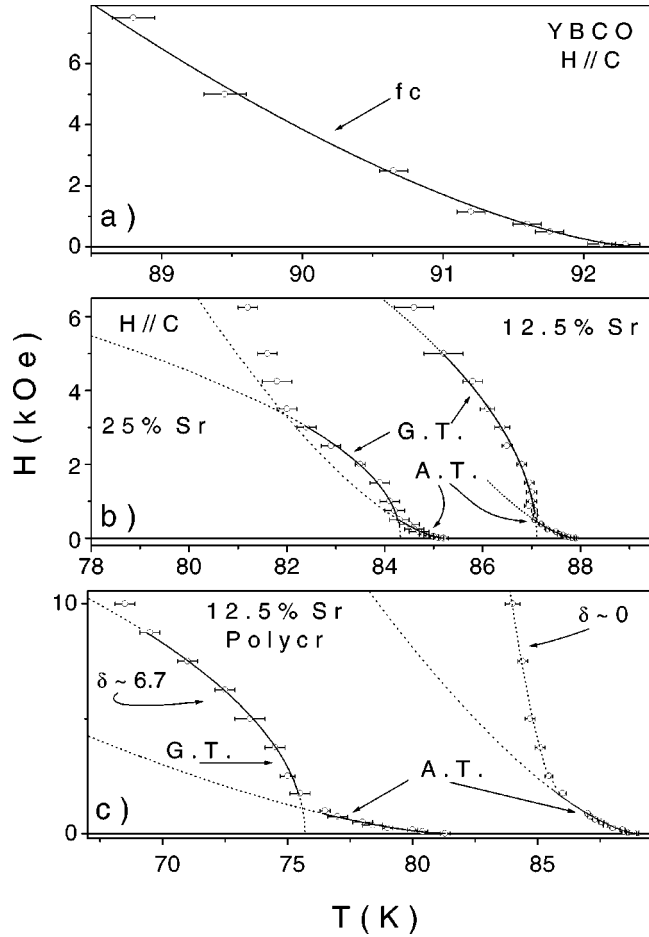


FIG. 5. The low-field details of the $T_{irr}(H)$ data of the pure single crystal (a), showing that the flux-creep (fc) line fits well the data down to zero field, the two Sr-doped single crystals (b), and the polycrystalline sample (c) in two oxygen states, showing systematically two different regimes. The continuous lines, indicated by AT or GT, are fitted with Eqs. (2) and (3), respectively (see fitting parameters in Table I). The dashed line is a guide to the eye.

field only shifts the phase of the GL order parameter along the transverse components of the weak links. The total phase displacement ΣA_{ij} along closed loops of grains is constrained to $2\pi f$, where f is an integer representing the total number of fluxons enclosed by the loop. The largely varying quality, the directional randomness of the junctions, and the consequent randomness of the phase factors A_{ij} together with the multiconnectedness of the grains leads to conflicting couplings, making it impossible to minimize the energy within all the grain junctions. The system becomes frustrated and its ergodicity breaks during freezing into a highly degenerate ground state with a very large number of nearly equal energy minima. By increasing the field the random-phase distortions A_{ij} debilitate even more the grain aggregate's ability to block the intergranular flux. Frustration of the grain couplings and the magnetic irreversibility in low fields are thus intimately connected. This is why measurements of flux dynamics and magnetic irreversibility in the granular superconductors can tell us so much about phase disorder and frustration.

TABLE I. The fitting parameters α , H_0 , and $T_{irr}(0)$ for the various regimes, as found for each sample, are indicated by fc for the high-field flux-creep regime and by AT and GT for the two low-field frustration dominated regimes.

Samples	Fit	α	H_0 (kOe)	$T_{irr}(0)$ (K)
YBa ₂ Cu ₃ O _{7-δ} (single crystal)	fc	1.50 ± 0.05	820.50	92.70
YBa _{1.75} Sr _{0.25} Cu ₃ O _{7-δ} (single crystal)	fc	1.49 ± 0.09	475.91	89.04
	GT	0.52 ± 0.05	25.57	87.15
YBa _{1.5} Sr _{0.5} Cu ₃ O _{7-δ} (single crystal)	fc	1.50 ± 0.08	583.70	85.40
	GT	0.50 ± 0.05	20.00	84.30
YBa _{1.75} Sr _{0.25} Cu ₃ O _{7-δ} (polycrystalline)	AT	1.52 ± 0.11	661.31	87.88
	AT	1.51 ± 0.05	465.70	85.20
YBa _{1.75} Sr _{0.25} Cu ₃ O _{6.7} (polycrystalline)	AT	1.49 ± 0.24	245.45	89.01
	AT	1.51 ± 0.05	57.40	81.40
YBa _{1.5} Sr _{0.25} Cu ₃ O _{6.7} (polycrystalline)	fc	1.51 ± 0.10	173.80	81.50
	GT	0.50 ± 0.05	30.30	75.70
YBa _{1.5} Sr _{0.25} Cu ₃ O _{6.7} (polycrystalline)	AT	1.51 ± 0.05	57.40	81.40

The vortex-glass approach examines the effect of the flux-line lattice distortions, caused by random pinning in the irregular topology of an inhomogeneous superconductor, on the correlation function between flux lines and the stability of a vortex-system as a whole. Due to the random flux pinning in the HTSC this theory predicts a transition from the vortex-liquid to a vortex-glass state at a well-defined glass temperature T_g . While the vortex-liquid phase is magnetically reversible, the vortex-glass is not. In reality the vortex-glass model is an alternative way to describe a disordered and frustrated superconductor.

The superconducting-glass and the vortex-glass models both simplify excessively the real problem of the inhomogeneous HTSC. While the first underestimates intragrain and spontaneous phase anisotropy effects, the second does not adequately incorporate the intergranular flux dynamics. Although both predict a glass transition along some well-defined line in the H - T plane, these lines are completely smooth and clearly cannot account for the systematic and remarkable details in the structure of our irreversibility lines. While a better theoretical approach lacks, we do our best comparing our $T_{irr}(H)$ results with those of the spin glasses that are intriguingly similar.

Another important observation is that in the low-field region of the H - T plane, where the Josephson flux dynamics is dominant, the irreversibility line $T_{irr}(H)$ runs well above the zero resistivity line $T_{C0}(H)$.¹⁹ This is in fact what is expected for a percolating superconducting grain network where $T_{irr}(H)$ occurs when the first grain loops close, while $T_{C0}(H)$ occurs at significantly lower temperature when about 15% of the grains are coupled.⁴⁵ Nevertheless in the high-field region, where the intragrain Abrikosov flux dynamics dominates, the $T_{irr}(H)$ and $T_{C0}(H)$ lines join together.⁴⁶

In conclusion, the $T_{irr}(H)$ data of our granular superconductors, besides identifying the intragrain Abrikosov flux dy-

namics in the major high-field region, apparently governed by the conventional flux-creep physics, they also clearly evidence the existence of a dominant intergranular Josephson flux dynamics in a low-field region that are strictly related to the granularity of our superconductors and characterized by AT- and GT-like lines. The AT and GT features in spin glasses represent a phase transition and are the well-known signature of frustration. The occurrence of precisely these features in our granular superconductors appoints disorder and frustration as the origin of these regimes. This also signals that the AT and GT features are not specific to frustrated spin systems but constitute a universality class that may congregate all the disordered and frustrated systems regardless

of the nature of the coupled objects. For the lack of a better theoretical approach, we suggest that the GT-AT crossover of $T_{irr}(H)$ for decreasing fields, present in our granular HTSC, is due to random-phase displacements, induced by the Coulomb term in the Hamiltonian, Eq. (4), which plays a role similar to the random anisotropy fields in the analogous crossover in spin glasses.²⁶

ACKNOWLEDGMENTS

The authors thank Dr. P. Pureur for putting contacts on the single crystal and to the Brazilian agencies CNPq, CAPES, and the PRONEX program for financial support.

-
- *Corresponding author. Instituto de Física - UFRGS Av. Bento Gonçalves, 9500 P.O. Box 15051, 91501-970 Porto Alegre - RS, Brazil. Email address: schaf@if.ufrgs.br
- ¹K.A. Müller, M. Takashige, and J.G. Bednorz, Phys. Rev. Lett. **58**, 1143 (1987).
- ²Y. Yeshurun and A.P. Malozemoff, Phys. Rev. Lett. **60**, 2202 (1988).
- ³P. Pureur, J. Schaf, and J.V. Kunzler, Prog. High Temp. Supercond. **9**, 137 (1988).
- ⁴J. Jung, M.A.K. Mohamed, I. Isaac, and L. Friedrich, Phys. Rev. B **49**, 12 188 (1994).
- ⁵P. Rodrigues, Jr., J. Schaf, and P. Pureur, Phys. Rev. B **49**, 15 292 (1994).
- ⁶J. Schaf, P. Pureur, and J.V. Kunzler, Phys. Rev. B **40**, 6948 (1989).
- ⁷G. Deutscher and K.A. Müller, Phys. Rev. Lett. **59**, 1745 (1987).
- ⁸M. Daeumling, J.M. Seuntjens, and D.C. Larbalestier, Nature (London) **346**, 332 (1990).
- ⁹K. Saito, H.U. Nissen, C. Beeli, T. Wolf, W. Schauer, and H. K pfer, Phys. Rev. B **58**, 6645 (1998).
- ¹⁰V. N. Vieira, J. Schaf, and P. Pureur, Physica C **353**, 241 (2001).
- ¹¹V.N. Vieira, P. Pureur, and J. Schaf, Physica C **354**, 299 (2001).
- ¹²P.W. Anderson and Y.B. Kim, Rev. Mod. Phys. **36**, 39 (1964).
- ¹³G. Blatter and B. Ivlev, Phys. Rev. Lett. **70**, 2621 (1993).
- ¹⁴A. Shilling, H.R. Ott, and Th. Wolf, Phys. Rev. B **46**, 14 253 (1992).
- ¹⁵H. Safar, P.L. Gammel, D.A. Huse, D.J. Bishop, J.P. Rice, and D.M. Ginsberg, Phys. Rev. Lett. **69**, 824 (1992).
- ¹⁶G.T. Seidler, T.F. Rosenbaum, D.L. Heinz, J.W. Downey, A.P. Paulikas, and B.W. Veal, Physica C **183**, 333 (1991).
- ¹⁷N.E. Hussey, H. Takagi, N. Mori, N. Takeshita, Y. Iye, S. Adachi, and T. Tanabe, J. Supercond. **12**, 583 (1999).
- ¹⁸D.A. Cardwell, N. Hari, W. Lo, and A.M. Campbell, Supercond. Sci. Technol. **13**, 646 (2000).
- ¹⁹J.P. da Silva, J. Schaf, P. Pureur, and S. Reich, Physica C **332**, 31 (1999).
- ²⁰W.Y. Shih, C. Ebner, and D. Stroud, Phys. Rev. B **30**, 114 (1984); *ibid.* **31**, 165 (1985).
- ²¹J.R. Rojas, R.M. Costa, P. Pureur, and P. Prieto, Phys. Rev. B **61**, 12 457 (2000).
- ²²G.G. Kenning, D. Chu, and R. Orbach, Phys. Rev. Lett. **66**, 2923 (1991).
- ²³J.R.L. de Almeida and D.J. Thouless, J. Phys. A **11**, 983 (1978).
- ²⁴J. Schaf, P. Pureur, and J.V. Kunzler, Prog. High Temp. Supercond. **25**, 262 (1990).
- ²⁵M. Gabay and G. Toulouse, Phys. Rev. Lett. **47**, 201 (1981).
- ²⁶G. Kotliar and H. Sompolinsky, Phys. Rev. Lett. **53**, 1751 (1984).
- ²⁷V.N. Vieira, J.P. da Silva, and J. Schaf, Physica C **341-348**, 1155 (2000).
- ²⁸F. Zuo, S. Khizroev, G.C. Alexandrakis, and V.N. Kopylov, Phys. Rev. B **52**, R755 (1995).
- ²⁹Y. Kopelevich, S. Moehlecke, and J.H.S. Torres, Phys. Rev. B **49**, 1495 (1994).
- ³⁰A. Schilling, R. Jin, J.D. Guo, and H.R. Ott, Phys. Rev. Lett. **71**, 1899 (1993).
- ³¹C.C. Almasan, M.C. de Andrade, Y. Dalichaouch, J.J. Neumeier, C.L. Seaman, M.B. Maple, R.P. Guertin, M.V. Kuric, and J.C. Garland, Phys. Rev. Lett. **69**, 3812 (1992).
- ³²X.G. Giu, V.N. Moshchalkov, and J. Karpinski, Phys. Rev. B **62**, 4119 (2000).
- ³³L. Ghivelder, I.A. Castillo, S. Salem-Sagui, Jr., R. de Andrade, Jr., M. Dhall , G. Grasso, F. Marti, and R. Fl kiger, Supercond. Sci. Technol. **12**, 566 (1999).
- ³⁴H. K pfer, Th. Wolf, A.A. Zhukov, and R. Meier-Hirmer, Phys. Rev. B **60**, 7631 (1999).
- ³⁵J.S. Chung, K.H. Lee, and D. Stroud, Phys. Rev. B **40**, 6570 (1989).
- ³⁶Z.Q. Wang and D. Stroud, Phys. Rev. B **44**, 9643 (1991).
- ³⁷K.H. Lee and D. Stroud, Phys. Rev. B **44**, 9780 (1991).
- ³⁸M.P.A. Fisher, Phys. Rev. Lett. **62**, 1415 (1989).
- ³⁹J. Toner, Phys. Rev. Lett. **67**, 2537 (1991).
- ⁴⁰D.A. Huse and H.S. Seung, Phys. Rev. B **42**, 1059 (1990).
- ⁴¹J.D. Reger, T.A. Tokuyasu, A.P. Young, and M.P.A. Fisher, Phys. Rev. B **44**, 7147 (1991).
- ⁴²A.T. Dorsey, M. Huang, and M.P.A. Fisher, Phys. Rev. B **45**, 523 (1992).
- ⁴³F.V. Kusmartsev, Phys. Rev. Lett. **69**, 2268 (1992).
- ⁴⁴B.I. Spivak and S.A. Kivelson, Phys. Rev. B **43**, 3740 (1991).
- ⁴⁵H. Scher and R. Zallen, J. Chem. Phys. **53**, 3759 (1970).
- ⁴⁶F.W. Fabris, J.R. Rojas, and P. Pureur, Physica C **354**, 304 (2001).